Journal of
Biomedical Engineering and Research

Research Open Access

Computational Modeling of Stent Implant Procedure and Comparison of Different Stent Materials

Karthik Alagarsamy[1], Aleksandra Fortier[1,*], Nilesh Kumar[2,3], Atif Mohammad[4], Subhash Banerjee[4], Hai-Chao Han[5], Rajiv S Mishra[2]

[1]Mechanical and Energy Engineering Department, College of Engineering, University of North Texas, Denton, TX, 76207 USA

[2]Materials Science and Engineering Department, College of Engineering, University of North Texas, Denton, TX, 76207

[3]Currently at: Department of Nuclear Engineering, College of Engineering, North Carolina State University, Raleigh, North Carolina, 27695

[4]Department of Internal Medicine, UT Southwestern Medical Center and VA North Texas Health Care System, Dallas, TX, 75390, USA

[5]Department of Mechanical Engineering, The University of Texas at San Antonio, San Antonio, Texas, 78249, USA

***Corresponding Author:** Aleksandra Fortier, Mechanical and Energy Engineering Department, University of North Texas, Denton, TX 76207, USA. E-mail: drafortier@gmail.com

Received Date: August 18, 2016, **Accepted Date:** September 23, 2016 **Published Date:** September 27, 2016

Citation: Karthik Alagarsamy (2016) Computational Modeling of Stent Implant Procedure and Comparison of Different Stent Materials. J Biomed Eng 1: 1-10.

Abstract

A stent in artery is subjected to significant mechanical loads due to the repetitive cyclical pressure loads and displacement of the artery wall. The arteries expands and contracts slightly as the pressure changes with the heart beat for long-term in-vivo service. The structure of the stent has to withstand these loads while scaffolding the narrow artery. Many different stent designs and materials have been studied. In our previous study [Alargasamy et. al. Mechanical properties of High Entropy Alloy Al0.1CoCrFeNi for Peripheral Vascular Stent Application, Cardiovascular Engineering and Technology] mechanical properties of High Entropy Alloy (HEA) are determined experimentally, the one to one comparison of these HEAs with stainless steel 316L was done. In this study in order to understand the behavior of HEA materials in actual stent implant application, the operation is simulated compuationally, using ANSYS Workbench, by applying stainless steel 316L and high entropy alloy properties as the material properties for the 3D stent model.

Keywords: High entropy alloys; Stent implants; Stainless steel; Peripheral stenting; 3D modeling; Finite element analysis; Superficial femoral artery

Introduction

High entropy alloys (HEAs) are new class of multi-component alloys with five or more principal elements each contributing 5 to 35 atomic percentage. The concept of HEA was first introduced in 1996 but extensive research started after 2004 when Jien-Wei Yeh and Brain Cantor published papers related to HEAs [1]. Literature reports on HEAs show unique properties such as improved strength, superior wear resistance, high temperature strength, improved fatigue and good corrosion resistance [1].

As a result of several metallic elements creating the HEA, presence of complex phase formation is common. Number of studies have been reported on microstructural characteristics and mechanical properties of various combinations of HEAs with lack of reports on their application [1,2]. Specifically, HEAs for biomedical application has not been reported to date. In this work we have selected to study the application of HEAs in peripheral vascular stent implants due to their 50% failure rate and need for base material that can potentially extend their life-cycle [3]. Heart disease is the leading cause of death among Americans, with about 600,000 deaths per year. Coronary heart disease alone kills more than 350,000/year and costs the United States about $110 billion each year [4].

This total includes the cost of health care services, medications, and lost productivity. In spite of significant advancement in clinical care and education to the public, cardiovascular diseases (CVD) prevail as the leading cause of death and disability. Cardiovascular disease is often related to atherosclerosis which can cause narrowing, rupture or erosion of the arterial wall, with eventual reduction or occlusion (i.e. 100% blockage) of blood flow in the artery. Among several different treatments is stent implant procedure, which is the insertion of a metal and/or plastic tubular structure that has the ability to expand into a cylindrical shape, either by use of balloon or a self-expansion mechanism. Stents are used as scaffolds to reopen vessels occluded from atherosclerosis, to close arterial dissections, or in case of covered stents for rechanneling blood through aneurysmal regions [5]. Although much stent research has focused on materials for coronary artery stents, this study focuses on the less studied field of materials for peripheral stenting found in the limbs of the human body, specifically in Superficial Femoral Artery (SFA) and their high failure rates [3,5]. It is reported that about 700,000 stent procedures (in coronary and peripheral arteries together) are done in the U.S. annually with about 50% stent failure rate in the SFA reported [4]. The SFA represents a harsh environment for stents, because mechanical forces such as bending, torsion, compression, and elongation can occur during the patient's daily activities. Despite the improvements in large stent materials available on the market the failure rates of peripheral vascular stents remain high and alternative design and/or material is needed [5]. In an effort to attack this problem, this paper discusses Al0.1CoCrFeNi HEA as a potential material for peripheral vascular stent application that can decrease stent failure rates. In general stents are classified into self-expanding and balloon expanding, based on how deployment is affected. A self-expanding stent is manufactured at the blood vessel diameter and they are compressed and constrained in a smaller diameter tube. Once it reaches the designated area the outer constrain is removed allowing the stent to reach the vessel diameter. A balloon-expanding stent is made in a crimped state and is expanded at the designated region by inflating it with a balloon. The stent reaches its plastic state and scaffolds the vessel and regulates the blood flow [6]. Doctors have proved that both self and balloon expanding stents can be used in cardiovascular and superficial femoral arteries. It is reported that the failure rate of stent in femoral artery located in thigh is higher due to the physical activities of the patient. Commercially used materials are stainless steel 316L and nitinol (NiTi alloy) for balloon expansion stents and cobalt-chromium alloys, titanium alloys and nitinol for self-expanding stents [7,8]. This study concentrates on reducing failure rates in peripheral balloon expanding stents as the stent is inflated by the balloon to its plastic state, materials with low yield stress are preferred [7,8]. Further, when choosing a material for medical implant application, biocompatibility of the material has to be assessed as the implants can cause adverse effect on the body. Co-Cr alloys, stainless steel, NiTi alloys, FeMn alloys are commonly used implants materials as they are bio compatible [9]. As a result, the HEA alloy content of Al0.1CoCrFeNi is assumed by the authors to be potentially biocompatible however, biocompatibility evaluation is beyond the scope of this paper. Experimental results reported in our previous work shows promising results for HEA as possible material for stent implants [10].

Therefore, in this study we further examine HEA compatibility by understanding the behavior of HEA materials in actual stent implant application. The stent implant operation is simulated compuationally, using ANSYS Workbench, by applying stainless steel 316L (the most common stent material) and high entropy alloy properties as the material properties for the 3D stent model.

Materials and Methods

Commonly used rhombus stent design was chosen for this modeling study as shown in Figure 1. By referring the basic stent model with 8 rhombus shape units the stent was modelled using SolidWorks.

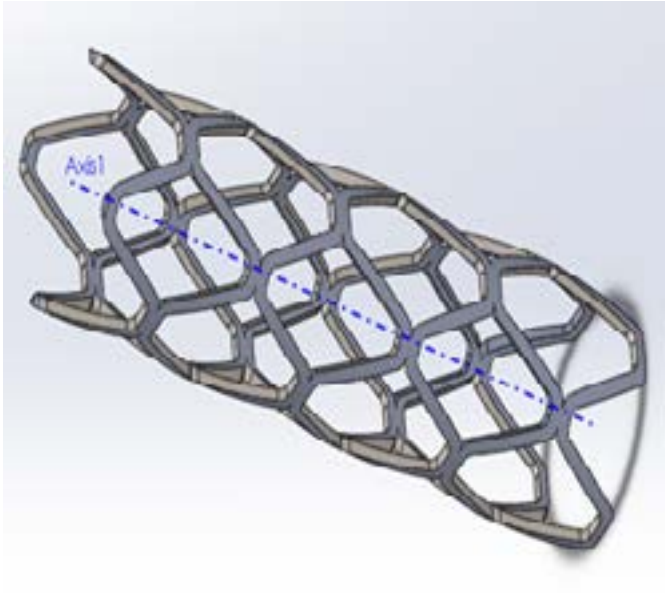

Figure 1: Rhombus structure of stent with 4 rhombus units – 8 struts [11].

Table 1 summarizes the dimensions of the stent that was used in modeling. The model is created and analyzed in ANSYS Workbench. This simulation is considered as a static structural analysis. The stents are modeled as linear elastic-plastic materials with bilinear isotropic hardening. Since the work is more concerned towards the properties of the stent, the balloon and artery are considered to be hyper-elastic materials. In the simulation, previously obtained properties [12] of stainless steel 316 L, CoCrFeNiMn and Al0.1CoCrFeNi HEA from literature or experimentally, were added as material properties to ANSYS Workbench materials library. Certain mechanical properties such tangent modulus, density, Poisson's ratio were calculated or referred from literatures. The tangent modulus which is the slope of the stress strain curve above the yield strength was calculated for the HEAs. In case of SS 316L the tangent modulus was considered as 0.01E [13]. The density which is mass divided by volume was also calculated by weighing samples and measuring their dimensions. The density and Poisson ratio of SS 316L was found to be 8000 kg/m3 and 0.3 respectively [14]. The Poisson ratio was assumed to be 0.3 for the HEAs.

Parameters	Values
Length	15 mm
Outer diameter	3.0mm
Strut width	0.05mm
Strut thickness	0.05mm
Longest diagonal of the rhombus	1.62mm
Shortest diagonal of the rhombus	1.18 mm
No. of units along circumference	8

Table 1: Dimensions of the stent model

Material	Yield strength MPa	Ultimate strength MPa	Young's modulus GPa	Tangent modulus GPa	Density kg/m3	Poisson's ratio
SS 316L	190	490	193	1.93	8000	0.3
CoCrFeNiMn	216	475	189	0.643	7954	0.3
$Al_{0.1}$ CoCrFeNi	212	570	203	0.843	7950	0.3

Table 2: Mechanical properties of SS 316L and Al0.1CoCrFeNi and CoCrFeNiMn HEAs added to ANSYS Workbench library

Table 2 summarizes the material and their mechanical properties that are added to the ANSYS Workbench library. The balloon was considered as hyperelastic Mooney-Rivlin 2 parameter model. The material constants C10, C01 and incompressibility parameter D1 was assigned as 1.06 MPa, 0.710MPa and 0 Pa-1 respectively [15]. The total geometry of the cylindrical stent was reduced by suppressing three out of the four quadrants and was considered as an axisymmetric model. The model was further reduced along the length to reduce the complexity of the analysis and also to reduce the computational time. The final CAD model of the stent was left with 4 rhombus units as shown in the Figure 2a.

The balloon was modelled along the inner radius of the stent using Workbench Geometry tool. The balloon with radius 1.45mm was extruded to 5 mm in such a way that the balloon covers the entire inner face of the stent. Figure 2b shows the design and dimension of the balloon. The SS 316L, CoCrFeNiMn and Al0.1CoCrFeNi material properties were applied for the stent and the hyperelastic property was applied to the balloon. A cylindrical coordinate system was created for the axisymmetric model.

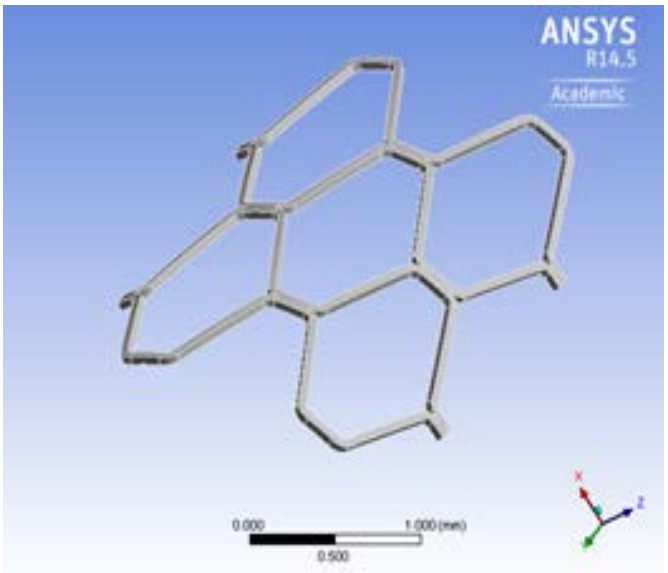

Figure 2: a) Reduced stent model used for axisymmetric structural analysis

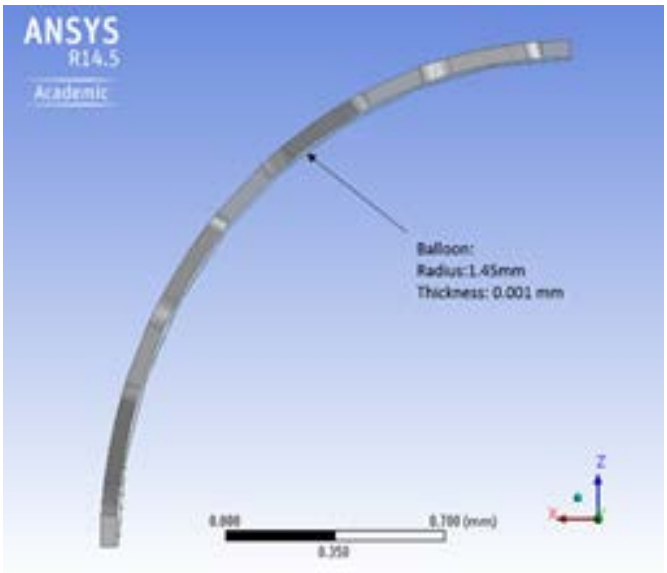

Figure 2: b) the reduced balloon model along the length

Figure 2c shows isometric view of the reduced stent and balloon model along with the cylindrical coordinate system. Defining contact parameters between surfaces is very important, so frictionless contact was defined between the upper surface of the balloon and inner surface of the stent.

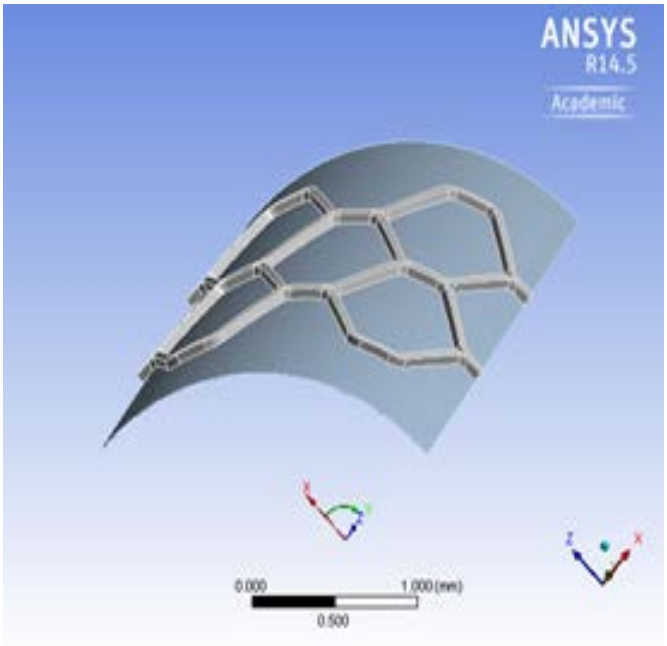

Figure 2: c) The reduced stent with balloon combined model used for axisymmetric structural analysis.

Figure 3a shows the contact faces of the stent and balloon. The model is meshed in the ANSYS Workbench Model tool. An element size of 0.04 mm was assigned for stent body and 0.05 mm for the balloon body. Mapped face mesh was assigned on the top surface of the balloon. Figure 3b shows the meshed stent and artery.

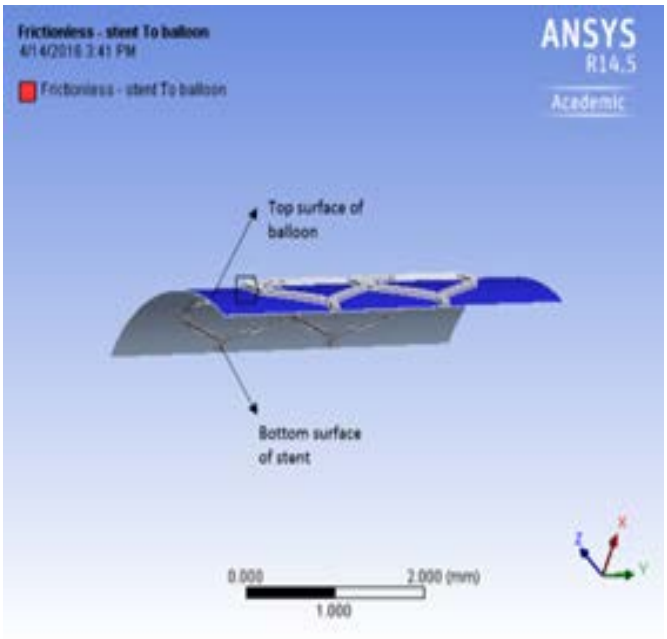

Figure 3: a) frictionless contact surfaces

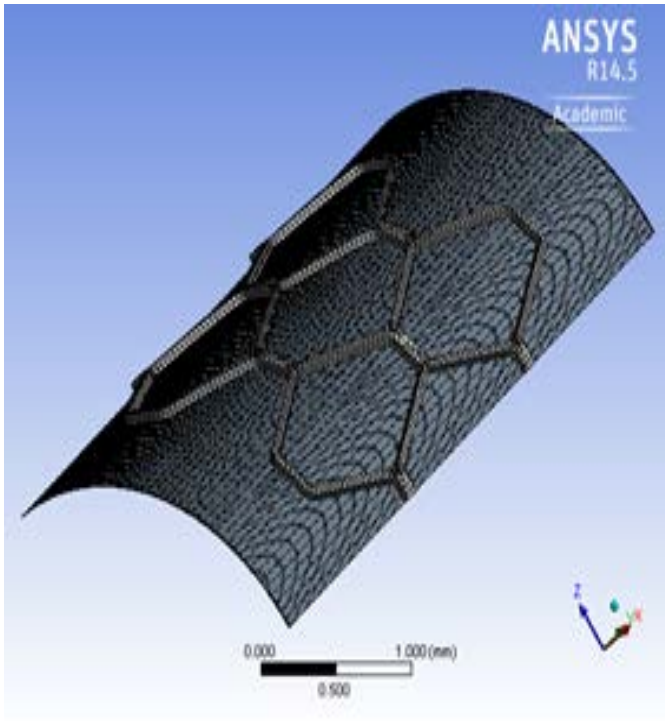

Figure 3: b) meshed stent and artery used for analysis

Boundary conditions were simulated as a step controlled model as it involves two steps. Step 1: Inflation of balloon that expands the stent and deforms it plastically and Step 2: Deflation of balloon leaving the stent in its deformed state. A displacement boundary condition was assigned to the inner surface of the artery. The balloon was deformed from 0 to 0.75 mm in the first step and then from 0.75 mm to 0 in the second step. Figure 4a shows the graph explaining the deformation boundary condition assigned to the balloon.

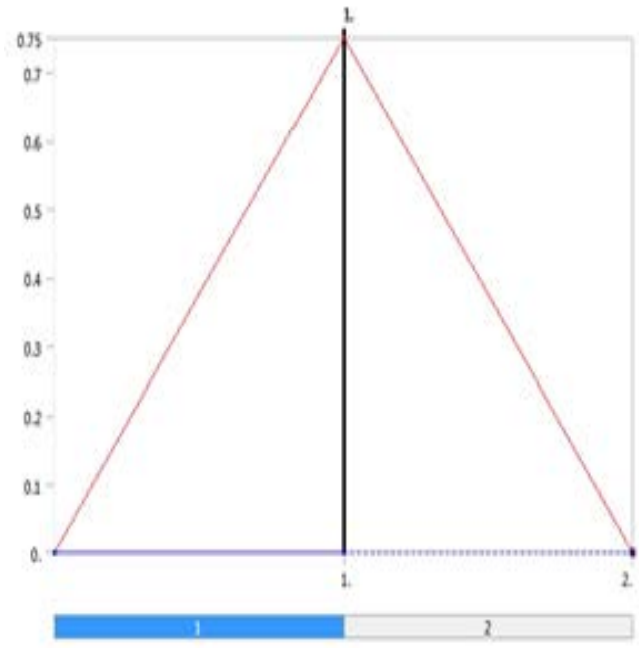

Figure 4: a) Graph showing the displacement boundary condition steps

Table 3 shows the displacement boundary condition applied for the inner surface of the balloon in the cylindrical coordinate system. Frictionless supports were applied on the 6 out of 8 faces around the corners of the stents to arrest the stent to rotate along Y direction and to arrest the displacement along Z direction. These supports just allows the stent to expand along X direction. Figure 4b shows the faces on which the frictionless support was applied.

Steps	Time [s]	X [mm]	Y [mm]	Z [mm]
1	0.	0.	0.	0.
	1.	0.75		
2	2.	0.	= 0.	= 0.

Table 3: Displacement boundary in cylindrical coordinate system for the balloon

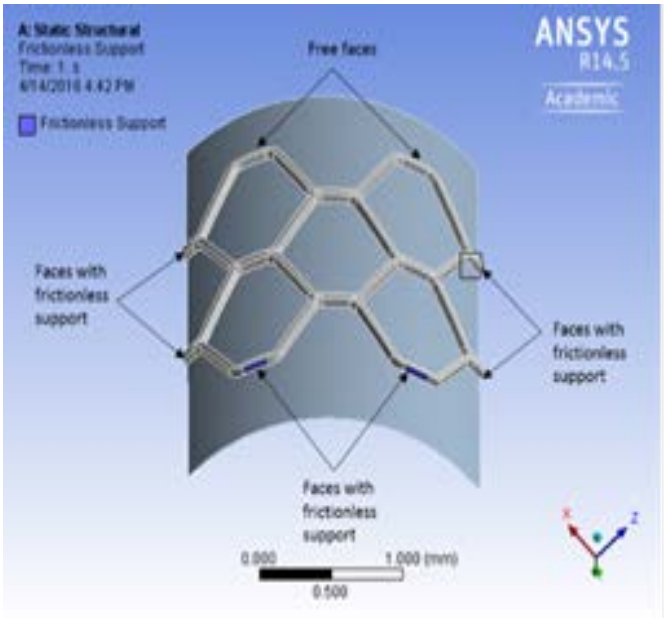

Figure 4: b) Free faces and faces with frictionless supports used in axisymmetric analysis

The solution for the 3 models with different stent materials (stainless steel 316L, Al0.1CoCrFeNi, and CoCrFeNiMn) produced results for the equivalent Von-Mises stress, total displacement and directional deformation of a point along X direction for each case. The results in form of graphs and graphical images were generated.

Results

All three models were analyzed for maximum equivalent Von-Mises stress, residual stress, maximum total displacement and directional displacement before and after recoil.

Model with Stainless steel 316L as stent material:

Figure 5 shows the maximum equivalent Von-Mises stress (at time 1) and residual stress (at time 2). The stent experiences maximum equivalent Von Mises stress of 410 MPa when the balloon expands completely as shown in Figure 5a.

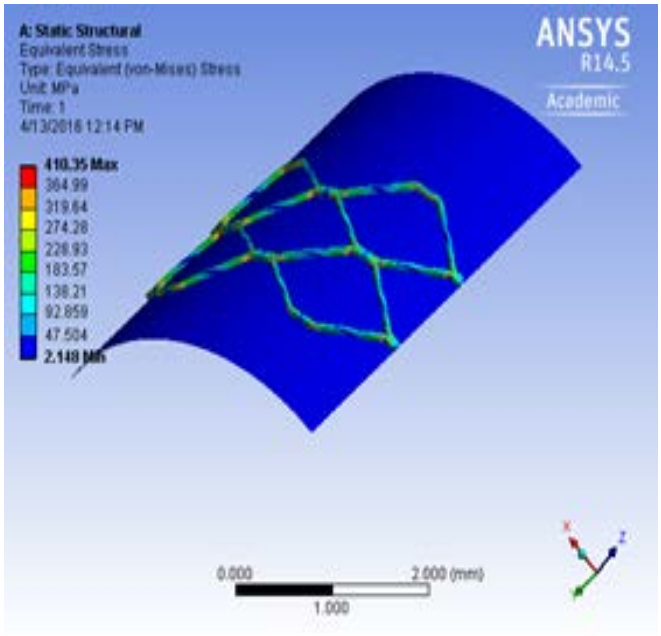

Figure 5 - SS 316L: a) Maximum equivalent Von Mises stress when the balloon is fully expanded

As the maximum equivalent stress is greater than the yield strength, the material reaches plasticity and does not regains its original shape when the balloon deflates. Thus when the balloon deflates, unloading occurs, the stress experienced by the stent drops and the contact between the stent and balloon breaks. The stent undergoes some amount recoiling and retains a maximum of 177 MPa in a form of residual stress as shown in figure 5b.

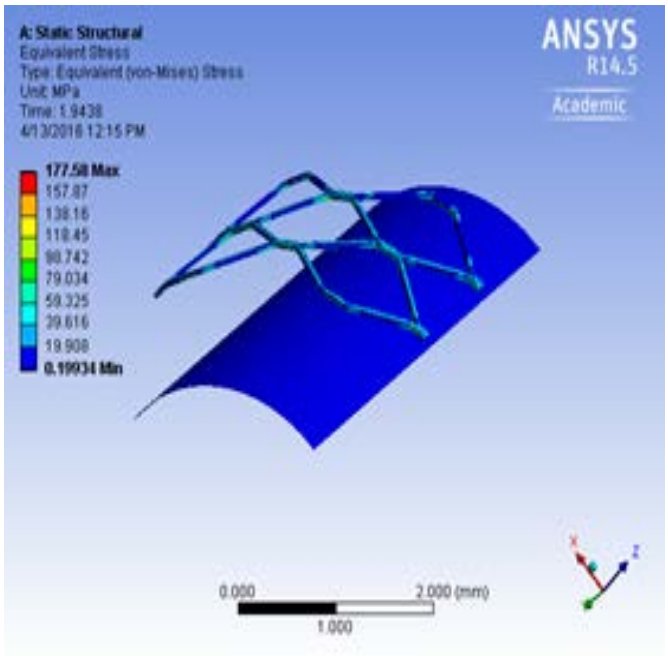

Figure 5: b) residual stress retained by the stent after deflation of balloon

The maximum total displacement and total displacement after recoiling during inflation and deflation of balloon is also shown. When the balloon is fully expanded, the unconstrained edges of the stent model undergoes a maximum total deformation of 1.156 mm and the minimum total displcement is 0.745 mm (Figure 5c).

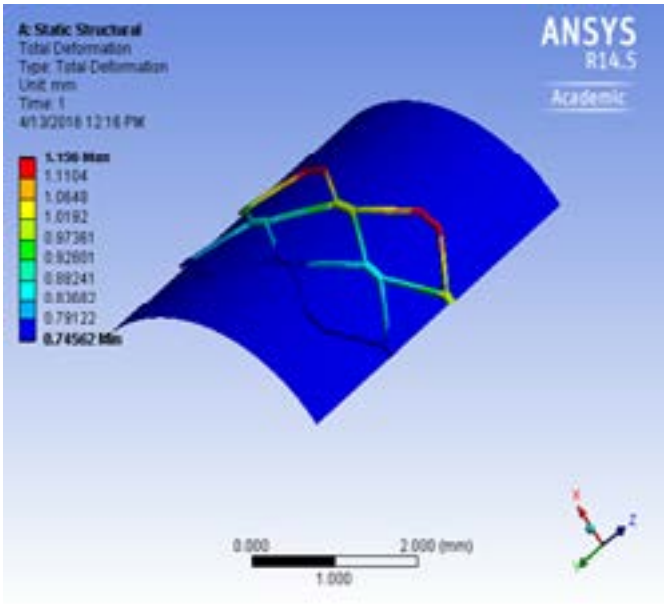

Figure 5: c) maximum total deformation at fully expanded condition

The total deflection deceases due to recoiling as the balloon deflates as shown in figure 5d.

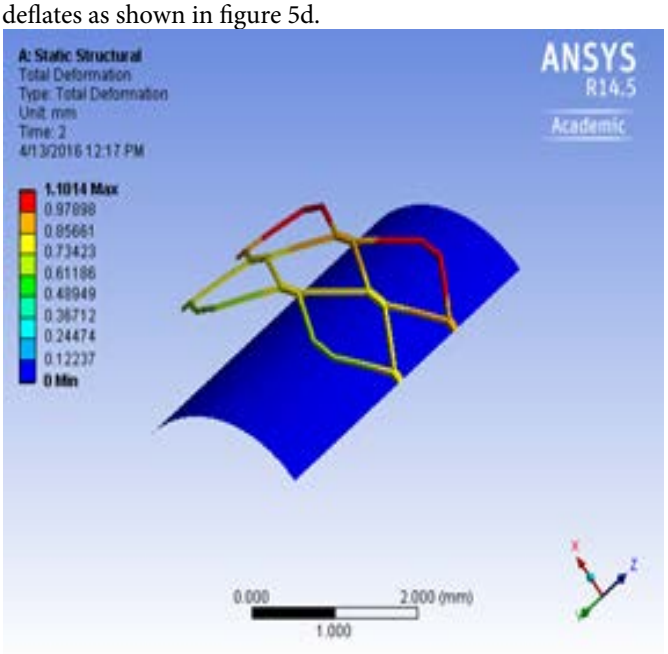

Figure 5: d) total deformation due to recoiling when the balloon deflates

The directional deformation of a point along X direction in the stent gives a clear idea about how the stent expands and recoils. In same Figure 5 the maximum displacement (at time=1) and displacement after recoil along the X direction (at time=2) is shown. The stent reaches a maximum displacement of 0.75325 mm along X direction at fully expanded balloon condition as shown in figure 5e.

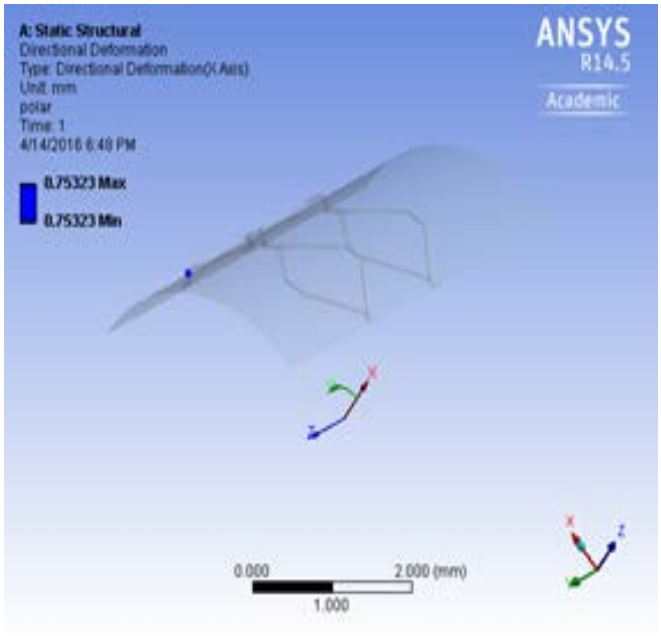

Figure 5: e) Maximum displacement along X at fully expanded balloon

When the balloon deflates the stent recoils and reaches 0.72567 mm as shown in figure 5f. Therefore the stent recoils about 0.028 mm (3.7%) along X direction.

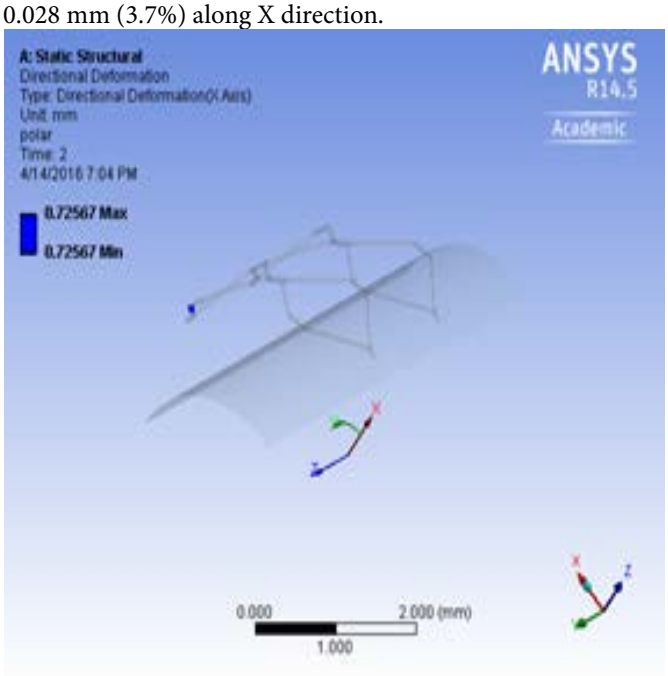

Figure 5: f) displacement along X after recoiling

Model with CoCrFeNiMn as stent material:

Figure 6 shows the maximum equivalent Von-Mises stress (at time 1) and residual stress (at time 2). The stent experiences maximum equivalent Von Mises stress of 323 MPa when the balloon expands completely as shown in Figure 6a. The stent reaches plastic state during loading.

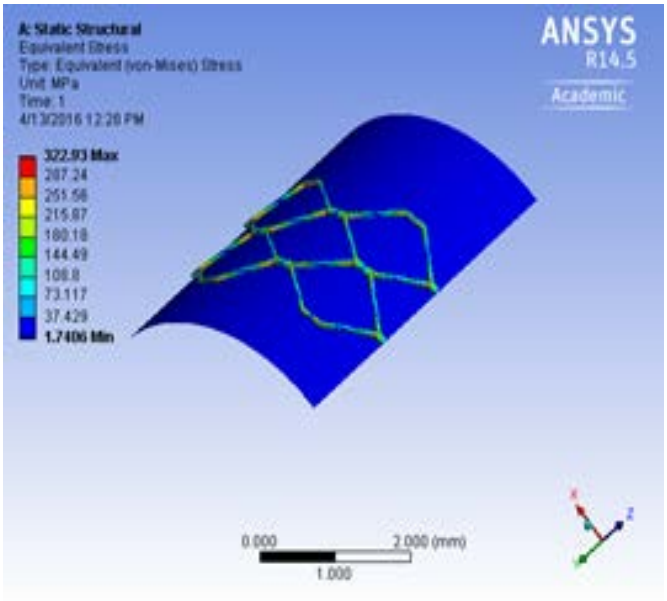

Figure 6 - CoCrFeNiMn: a) Maximum equivalent Von Mises stress when the balloon is fully expanded

During unloading the stent undergoes some amount recoiling and retains a maximum of 193 MPa in a form of residual stress as shown in figure 6b.

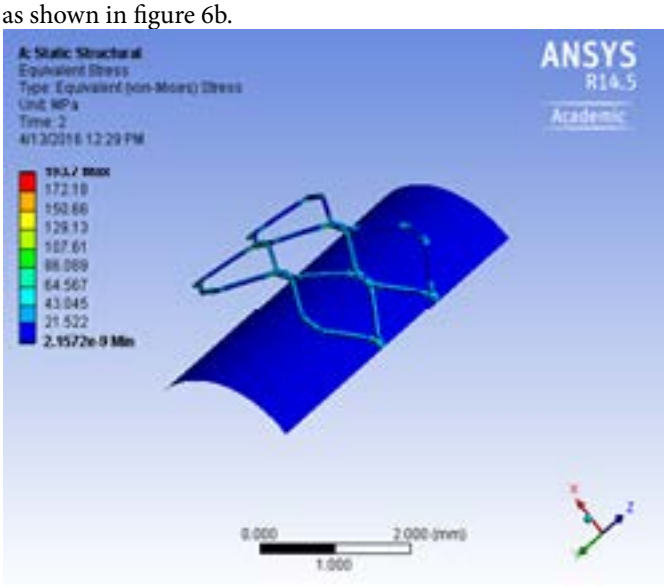

Figure 6: b) residual stress retained by the stent after deflation of balloon

The maximum total deformation and total deformation after recoiling when the balloon innflates and deflates is also shown. When the balloon is fully expanded, the unconstrained edges of the stent model undergoes a maximum total deformation of 1.161 mm and the minimum total displcement is 0.745 mm as shown in figure 6c. The total deflection deceases due to recoiling as the balloon deflates as shown in figure 6d. The maximum displacement (at time=1) and displacement after recoil along the X direction (at time=2) is shown. The stent reaches a maximum displacement of 0.75369 mm along X direction at fully expanded balloon condition as shown in figure 6e. When the balloon deflates the stent recoils and reaches 0.72927 mm as shown in figure 6f. Therefore the stent recoils about 0.024 mm (3.2%) along X direction.

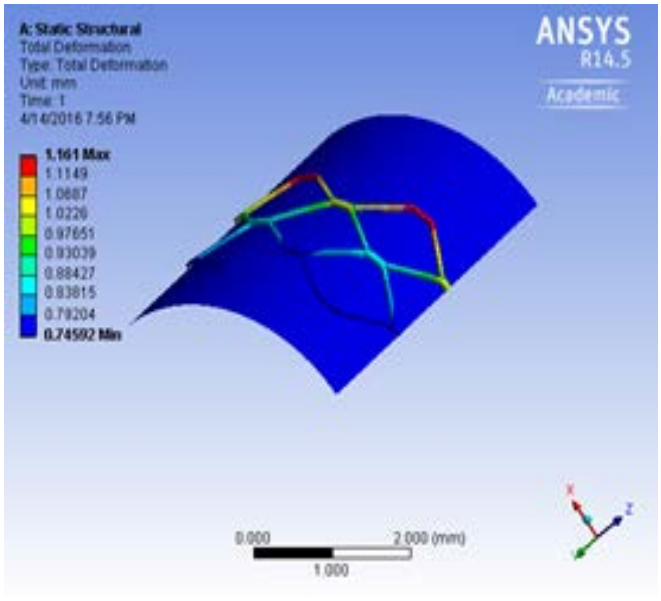

Figure 6: c) maximum total deformation at fully expanded condition

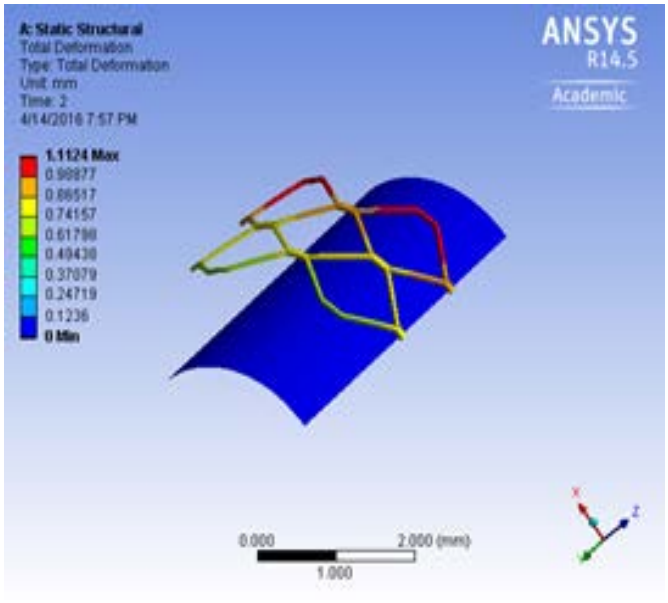

Figure 6: d) total deformation due to recoiling when the balloon deflates

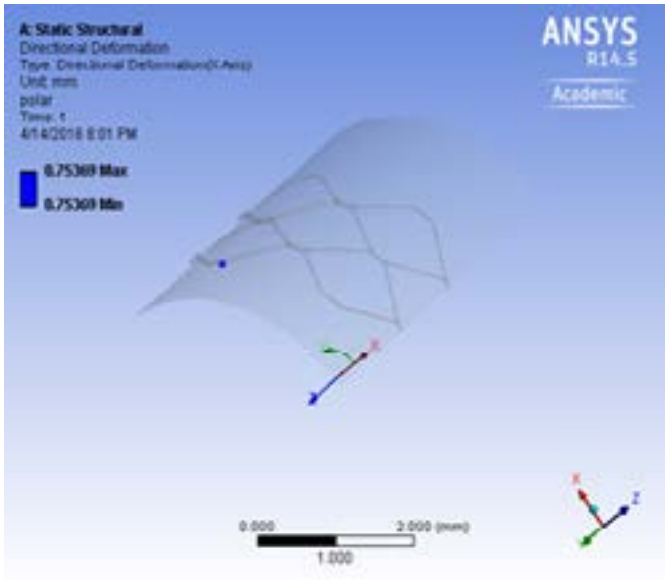

Figure 6: e) Maximum displacement along X at fully expanded balloon

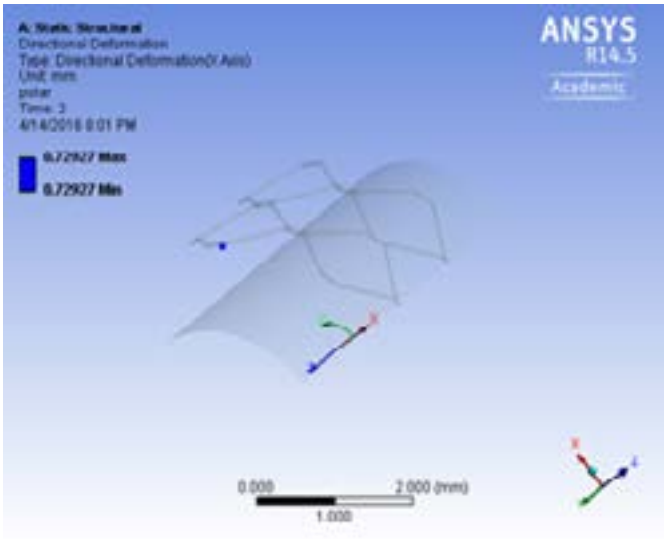

Figure 6: f) displacement along X after recoiling.

Model with Al0.1CoCrFeNi as stent material:

Figure 7 shows the maximum equivalent Von-Mises stress (at time 1) and residual stress (at time 2). The stent experiences maximum equivalent Von Mises stress of 345 MPa when the balloon completely expands as shown in Figure 7a. The stent reaches plastic state during loading. During unloading the stent undergoes some amount recoiling and retains a maximum of 191 MPa in a form of residual stress as shown in figure 7b. The maximum total deformation and total deformation after recoiling during inflation and deflation of the balloon is also shown. When the balloon is fully expanded, the unconstrained edges of the stent model undergoes a maximum total deformation of 1.1596 mm and the minimum total displcement was 0.745 mm as shown in figure 7c. The total deflection deceases due to recoiling as the balloon deflates as shown in figure 7d. The directional deformation of a point along X direction in the stent gives a clear idea about how the stent expands and recoils. Figure 7 shows the maximum displacement (at time=1) and displacement after recoil along the X direction (at time=2). The stent reaches a maximum displacement of 0.75358 mm along X direction at fully expanded balloon condition as shown in figure 7e. When the balloon deflates the stent recoils and reaches 0.72978 mm as shown in figure 7f. Therefore the stent recoils about 0.0238 mm (3.1%) along X direction.

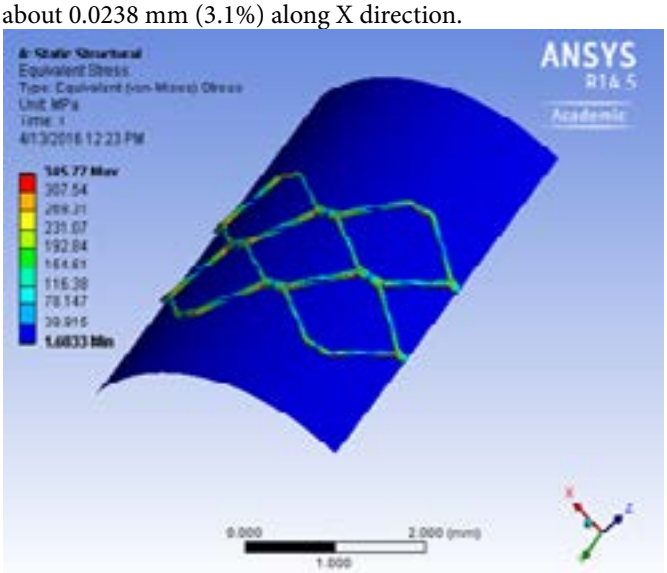

Figure 7 - Al0.1CoCrFeNi: a) Maximum equivalent Von Mises stress when the balloon is fully expanded

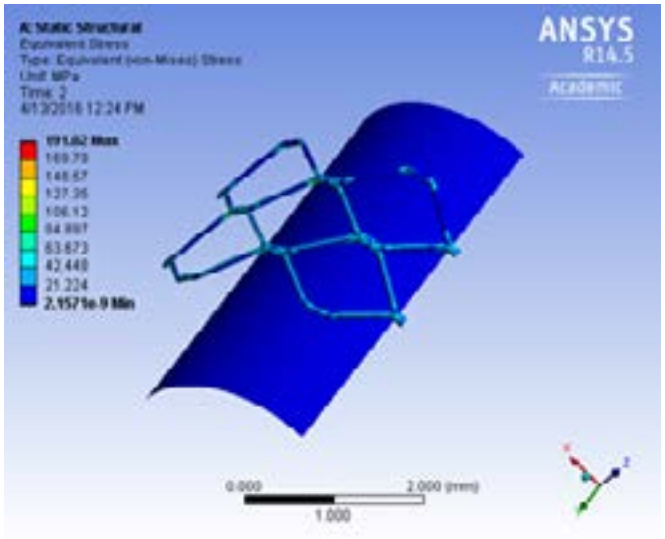

Figure 7: b) residual stress retained by the stent after deflation of balloon

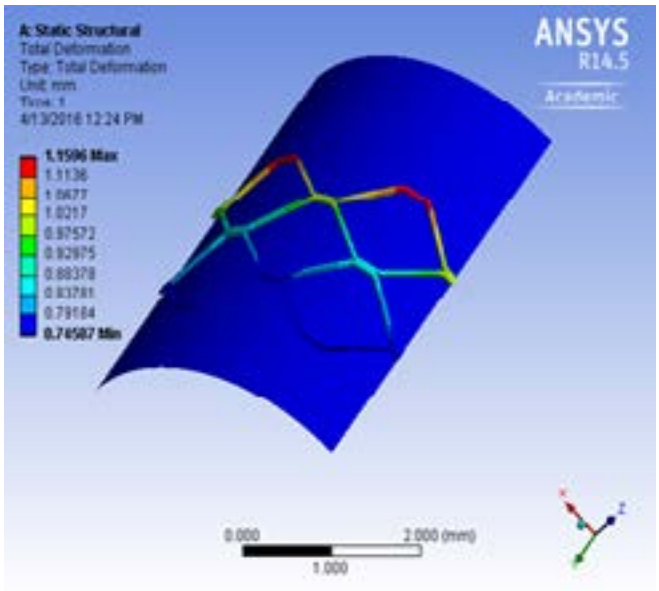

Figure 7: c) maximum total deformation at fully expanded condition

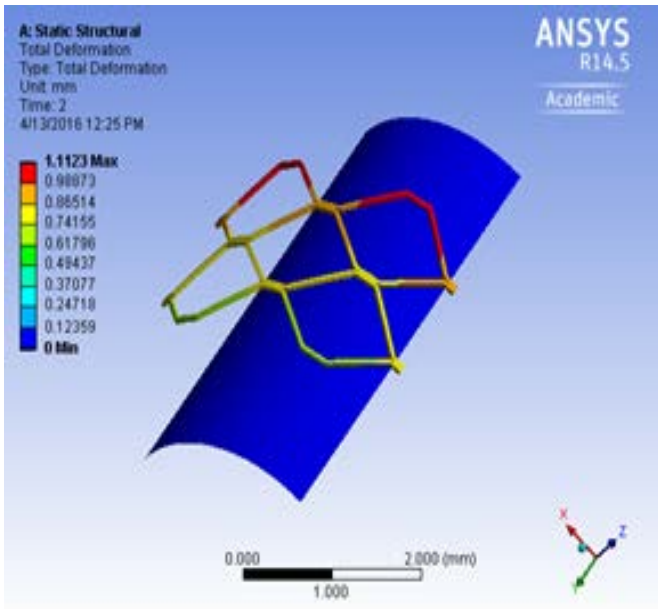

Figure 7: d) total deformation due to recoiling when the balloon deflates

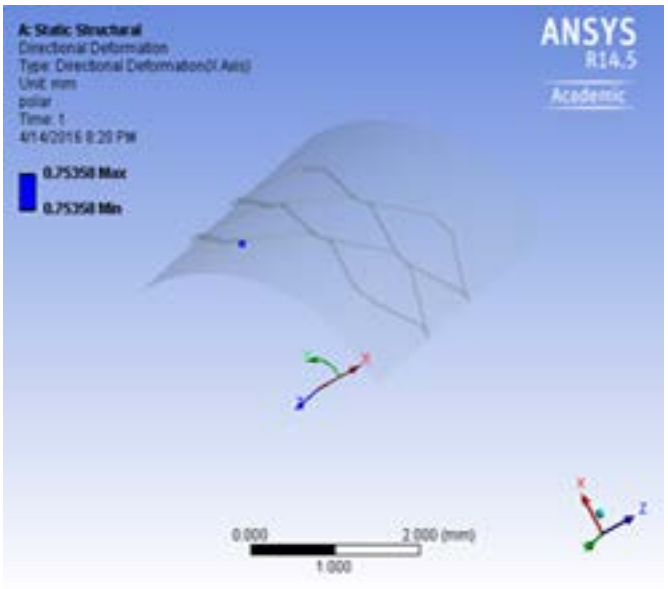

Figure 7: e) Maximum displacement along X at fully expanded balloon

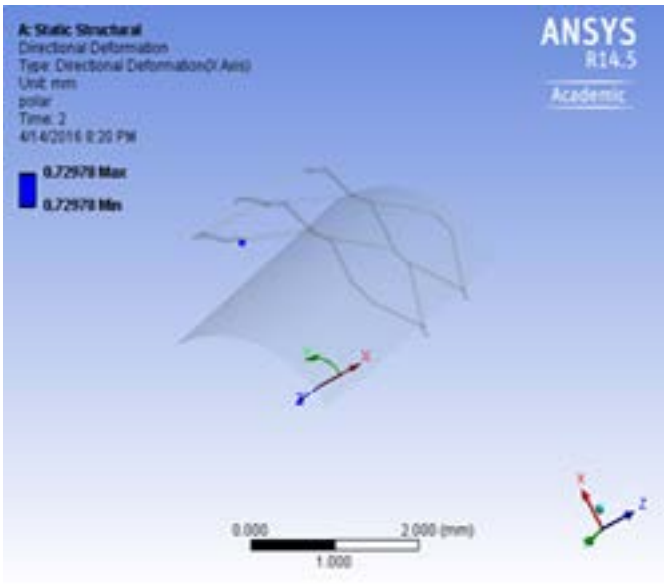

Figure 7: f) displacement along X after recoiling.

Discussions

The computational FEM analysis was done using ANSYS Workbench. A stent with rhombus structural unit and a hyperelastic balloon was modelled for the analysis. The mechanical properties of stainless steel 316L and experimentally determined mechanical properties of the high entropy alloys were assigned to the stent model. Static structural analysis was carried out in two steps to simulate the inflation and deflation of balloon. The equivalent Von Mises stress, total deformation and recoiling characteristics of the HEAs and stainless steel 316L were determined and compared. From the computational FEM analysis it was found that the structural behavior of the HEAs are same as stainless steel. Thus from the experimental and computational analysis and comparison of HEAs and stainless steel 316L, it was found that the HEAs has great potential to be used as stent materials. Though some mechanical properties were closely matching, the endurance limit of HEAs are found to be superior to stainless steel. This infers that the fatigue life of the stent will improve considerably when high entropy alloy are used as base material.

Table 4 compares the results generated from the computational analysis of all three materials. From the comparison it was found that the stainless steel experiences maximum stress while loading and it also possess higher recoils percentage.

Material	Max Von Mises stress MPa	Max residual stress MPa	Max total deformation mm	Recoil percentage %
SS 316L	410	177	1.156	3.7
CoCrFeNiMn	323	193	1.161	3.2
$Al_{0.1}$ CoCrFeNi	345	191	1.596	3.1

Table 4: Summary of results generated from computational analysis

From the results, it is evident that the Stainless steel 316L is flexible compared to the HEAs but not by a larger margin which means that HEAs have potential to be used as an alternate material for stainless steel 316L. The future work will concentrate more on computational fatigue analyses of stent when subjected to cyclic loads. The stent when implanted in artery undergoes cyclic load due to the systolic and diastolic pressure caused during heartbeat. Structural and fatigue analysis will be conducted by considering these the balloon expansion and cyclic pressure/load acting on the stent due to heart beat to further test HEA for stent application.

Acknowledgments

This work was supported by internal funds from UNT. We thank the team at UTSW Medical Center for providing valuable feedback and inspiring us to perform more research on stent implants. Authors would like to also thank Dr. Fanrong Kong for providing technical guidance and valuable discussions. All authors equally contributed to this manuscript.

References

1) Ming-Hung Tsai, Jien-Wei Yeh (2014) High-Entropy Alloys: A Critical Review. Materials Research Letters 3: 107-123.

2) Yong Zhang, Ting TingZuo, Zhi Tang, Michael C Gao, Karin A, et al. (2014) Microstructure and properties of high entropy alloys. Progress in Materials Science 61: 1-93.

3) Banerjee S, Das TS, Abu-Fadel MS, Dippel EJ, Shammas NW, et al. (2012) Pilot trial of cryoplasty or conventional balloon post-dilation of nitinol stents for revascularization of peripheral arterial segments: the COBRA trial. J Am CollCardiol 15: 1352-1359.

4) Rosamond W, Flegal K, Furie K, Go A, Greenlund K, et al. (2008) American Heart Association Statistics Committee, and Stroke Statistics Subcommittee Heart disease and stroke statistics--2008 update: a report from the American Heart Association Statistics Committee and Stroke Statistics Subcommittee. Circulation 4: 25-146.

5) A Fortier, V Gullapalli, R A Mirshams (2014) "Review of Biomechanical Studies of Arteries and Their Effect on Stent Performance". IJC Heart and Vessels 4: 12-18.

6) Robbins SL, Vinay K (2010) "Robbins and Cotran pathologic basis of disease". (8th edn) Saunders/Elsevier, Philadelphia.

7) T W Duerig, M Wholey (2002) A Comparison of Balloon- and Self- Expanding Stents. Min InvasTher& Allied Technol 4: 173-178.

8) Stoeckel D, Bonsignore C, Duda S (2002) A Survey of Stent Designs. Min Invas Ther & Allied Technol 4: 137-147.

9) D Mihov, B Katerska (2010) Some Biocompatible materials used in medical practice, Trakia Journal of Sciences 8: 119-125.

10) Alagarsamy K, Fortier A, Komarasamy M, Kumar N, Mohammad A, et al. (2016) "Mechanical properties of High Entropy Alloy Al0.1CoCrFeNi for Peripheral Vascular Stent Application". Cardiovascular Engineering and Technology.

11) H Yang (2015) "Study of Mechanical Performance Of Stent Implants Using Theoretical & Numerical Approach". University of North Texas, Denton, TX, U.S.A.

12) Alagarsamy K (2016) "Application of High Entropy Alloys in Stent Implants", University of North Texas, Denton, TX U.S.A.

13) S Shankar, M M Mayuram (2008) Effect of Strain Hardening in Elastic-Plastic Transition Behavior in a Hemisphere in contact with a Rigid Flat. International Journal of Solids and Structures 45: 3009-3020.

14) http://www.efunda.com/materials/alloys/stainless_steels/show_stainless.cfm?ID=AISI_Type_316L&prop=all&Page_Title=AISI%20Type%20316L

15) S N David Chua, B J MacDonald a, M S J Hashmi (2003) Finite Element Simulation of Stent and Balloon Interaction. J. Mater. Process. Technol 144: 591-597.